IGFBP7 Binds to the IGF-1 Receptor and Blocks Its Activation by Insulin-Like Growth Factors

Valentina Evdokimova,[1,2] Cristina E. Tognon,[3] Tania Benatar,[1] Wenyi Yang,[1] Konstantin Krutikov,[1] Michael Pollak,[4] Poul H. B. Sorensen,[3,5] Arun Seth[1]*

Insulin-like growth factor–binding protein 7 (IGFBP7) is a secreted factor that suppresses growth, and the abundance of IGFBP7 inversely correlates with tumor progression. Here, we showed that pretreatment of normal and breast cancer cells with IGFBP7 interfered with the activation and internalization of insulin-like growth factor 1 receptor (IGF1R) in response to insulin-like growth factors 1 and 2 (IGF-1/2), resulting in the accumulation of inactive IGF1R on the cell surface and blockade of downstream phosphatidylinositol 3-kinase (PI3K)–AKT signaling. Binding of IGFBP7 and IGF-1 to IGF1R was mutually exclusive, and the N-terminal 97 amino acids of IGFBP7 were important for binding to the extracellular portion of IGF1R and for preventing its activation. Prolonged exposure to IGFBP7 resulted in activation of the translational repressor 4E-binding protein 1 (4E-BP1) and enhanced sensitivity to apoptosis in IGF1R-positive cells. These results support a model whereby IGFBP7 binds to unoccupied IGF1R and suppresses downstream signaling, thereby inhibiting protein synthesis, cell growth, and survival.

INTRODUCTION

Insulin-like growth factor 1 receptor (IGF1R) and insulin receptor (INSR) are ubiquitous in normal cells and tissues and play critical roles in regulating growth, differentiation, survival, longevity, and metabolism (*1*–*3*). There is now considerable evidence that IGF1R and the signal transduction networks it regulates have important roles in neoplasia that make it an attractive therapeutic target (*3*–*5*). However, therapeutic targeting of IGF1R is complicated by its extensive crosstalk with INSR and by oncogenic activation of other alternative signaling pathways that converge downstream of IGF1R (*3*, *5*–*8*). IGF1R and INSR are structurally similar. Both consist of two half-receptors, each composed of one extracellular α-subunit responsible for ligand binding and one predominantly intracellular β-subunit with tyrosine kinase activity. The α and β subunits are generated from single precursor molecules. Because of high sequence similarity, IGF1R and INSR can form hybrid receptors, in which insulin half-receptors associate with IGF half-receptors (*1*, *9*). IGF1R and INSR are activated by the binding of their ligands IGF-1 or IGF-2 and insulin, respectively, resulting in the autophosphorylation of several tyrosine residues within their β subunits and subsequent recruitment of insulin receptor substrate-1 (IRS-1) and IRS-2, as well as other proteins. In turn, IRS proteins activate downstream phosphatidylinositol 3-kinase (PI3K)–AKT and Ras–mitogen-activated protein kinase (MAPK) signaling pathways (*1*, *2*, *4*).

The activities of IGF1R and INSR are tightly regulated at multiple levels, including their processing, endocytosis, and trafficking, and the bioavailability of their cognate ligands (*1*, *4*). The latter is controlled in part by the family of secreted IGF-binding proteins (IGFBP1 to IGFBP6), which have high affinity for IGF-1. In addition, various IGFBP-related proteins have been identified (*10*, *11*). IGFBP7, also known as IGFBP-related protein 1 (IGFBP-rP1), mac25, prostacyclin-stimulating factor (PSF), tumor adhesion factor (TAF), or angiomodulin (AGM), shares ~30% similarity with IGFBP1 to IGFBP6 in its N-terminal domain, including the conserved IGFBP motif, and is thought to function predominantly as a tumor suppressor (*12*). IGFBP7 binds to insulin, IGF-1, and IGF-2; however, its affinity for IGF-1 is more than 100-fold lower than that of IGFBP1 to IGFBP6 (*11*, *13*). Although IGFBP7 has been shown to enhance IGF-1 and insulin activities by stimulating growth of mouse fibroblasts (*14*), other studies have suggested that it blocks INSR activation by binding to insulin (*15*) or that it functions in an IGF- and insulin-independent manner (*16*). Here, we tested the role of IGFBP7 in regulating IGF1R and INSR signaling in normal and cancerous mammary epithelial cell lines and *Igf1r*-null mouse fibroblasts. We established that in contrast to IGFBP1 to IGFBP6, which reduce IGF1R activity by sequestering IGFs (*10*), IGFBP7 directly binds to IGF1R and blocks its activation. Prolonged exposure to IGFBP7 enhanced IGF1R protein stability and induced apoptosis in an IGF1R-dependent manner, indicating that IGFBP7 may protect IGF1R from degradation in the absence of its ligands while suppressing its growth and survival activities.

RESULTS

IGFBP7 blocks IGF1R activation in normal and breast cancer cells

We sought to determine the effect of IGFBP7 on signaling downstream of IGF1R and INSR in normal and breast cancer cells. We expected that if IGFBP7 could bind to insulin, IGF-1, or both as previously suggested (*13*–*15*), it would interfere with IGF1R or INSR-mediated signaling induced by these ligands. For our initial analysis, we chose MCF10A cells, a nontransformed cell line that recapitulates many properties of normal mammary epithelium, and MCF10CA1a cells, an H-Ras–transformed, highly malignant and metastatic subclone (*17*). When added simultaneously with insulin, IGF-1, or IGF-2, IGFBP7 did not affect the phosphorylation of IGF1Rβ or INSRβ or the activation of downstream PI3K-AKT signaling induced by these factors (fig. S1), arguing against the notion that IGFBP7 sequesters receptor ligands into inactive complexes. In contrast, pretreatment with IGFBP7 in serum-free medium significantly reduced subsequent

[1]Biological Sciences Platform, Sunnybrook Research Institute and Department of Laboratory Medicine and Pathobiology, University of Toronto, Toronto, Ontario M4N 3M5, Canada. [2]Institute of Protein Research, Pushchino, Moscow Region 142290, Russian Federation. [3]Department of Molecular Oncology, British Columbia Cancer Research Centre, Vancouver, British Columbia V5Z 1L3, Canada. [4]Departments of Medicine and Oncology, McGill University and Jewish General Hospital, Montreal, Quebec H3T 1E2, Canada. [5]Department of Pathology, University of British Columbia, Vancouver, British Columbia V5Z 4H4, Canada.
*To whom correspondence should be addressed. E-mail: arun.seth@utoronto.ca

IGF-1– or insulin-induced phosphorylation of IGF1Rβ or INSRβ in both MCF10A and MCF10CA1a cell lines (Fig. 1, A and B). IGF-1–induced phosphorylation of IGF1Rβ or INSRβ was also inhibited in BT474 cells and, to a lesser extent, in MDA-MB231 breast cancer cell lines (fig. S2A). Although the response of IGF1Rβ to IGF-1 was almost completely blocked, phosphorylation of AKT was less affected in IGFBP7-treated MCF10CA1a cells (Fig. 1, A and B). Likewise, phosphorylation of AKT in Hs578T cells was not affected by IGFBP7 treatment, potentially because of the low abundance of IGF1R and INSR and constitutive activation of AKT signaling (fig. S2A) (*18*). In both MCF10CA1a and Hs578T cells, AKT signaling is likely driven by the activated Ras-MAPK pathway because oncogenic H-Ras mutants are present in both cell lines [the G12V mutant in MCF10CA1a cells (*17*) and the G12D mutant in Hs578T (*19*)]. Together, these results indicate that in the absence of their cognate ligands, IGFBP7 can specifically target IGF1R or INSR but does not block alternative pathways such as Ras-MAPK that may also activate AKT signaling.

Given that the high doses of insulin (10 μg/ml; 2 μM) used in the above experiments can induce phosphorylation of IGF1Rβ in MCF10A cell lines (*20*, *21*), we set out to determine whether IGF1R or INSR was most affected by IGFBP7. To uncover early activating events, we analyzed MCF10A cells pretreated with IGFBP7, 5 min after induction with insulin, IGF-1, or IGF-2. Phosphorylation of IGF1Rβ and AKT remained low in IGFBP7-treated cells even in the presence of the highest concentrations of the corresponding IGFs (Fig. 1C). In contrast, insulin-induced phosphorylation of AKT and Ras–extracellular signal–regulated kinase (ERK) signaling appeared to be less affected by IGFBP7 (Fig. 1C). Immunoprecipitation results further confirmed that IGFBP7 prevents IGF-1–induced phosphorylation of IGF1Rβ and binding of the downstream scaffold protein IRS-1 but did not affect insulin-induced phosphorylation of INSRβ and IRS-1 binding (Fig. 1D).

Despite the inability of IGFBP7 to block constitutively active AKT signaling in certain cell lines, treatment with IGFBP7 efficiently suppressed IGF-1–induced phosphorylation of IGF1Rβ in all cell lines analyzed in this study. Moreover, ectopic expression of the secreted form of IGFBP7 in MDA-MB468 cells also blocked activation of IGF1R in response to IGF-1 (fig. S2B). Similar to MCF10CA1a and Hs578T cells, however, IGFBP7 did not prevent downstream phosphorylation of AKT, which was persistently high in serum-starved and IGF-1– or insulin-stimulated MDA-MB468 cells (fig. S2, A and C), likely because of inactivating *PTEN* mutations and *EGFR* amplifications in this cell line (*19*, *22*). IGFBP7 did not interfere with insulin-induced phosphorylation of INSRβ, which was enhanced in MDA-MB468 cells expressing IGFBP7 compared to vector-alone cells (fig. S2B), suggesting that in some cell lines, IGFBP7 may actually induce INSR activity. This could be due to a compensatory response to the IGF1R blockade because the same phenomenon has been observed with specific IGF1R inhibitors (*23*, *24*). These results demonstrate that externally added or ectopically expressed IGFBP7 potently and selectively inhibits the activity of IGF1R.

IGFBP7 suppresses the internalization of IGF1R in response to IGF-1 and increases IGF1Rβ protein stability

In cells ectopically expressing IGFBP7 and in IGFBP7-treated cells, immunofluorescence microscopy and cell fractionation indicated that large amounts of the protein were associated with the plasma membrane (fig. S3), consistent with previous reports (*12*, *25*, *26*). We investigated whether

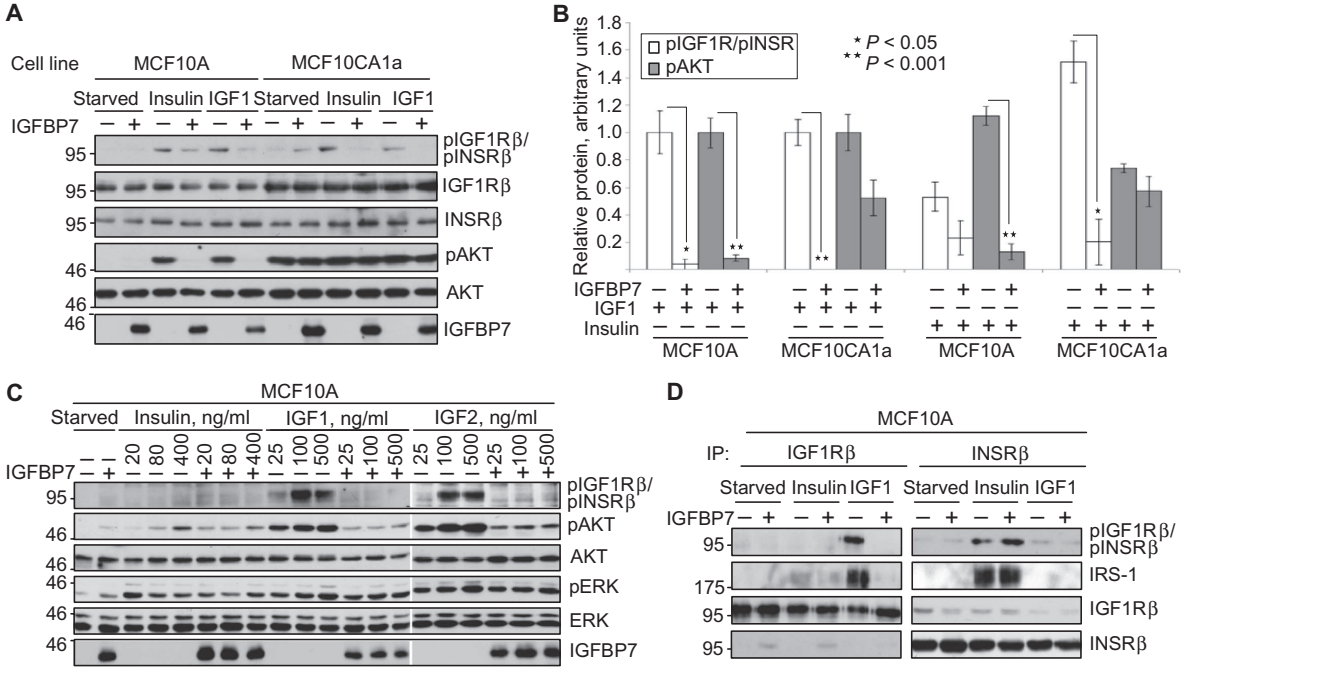

Fig. 1. IGFBP7 blocks IGF1R activation in mammary epithelial cells. (**A**) Serum-starved MCF10A and MCF10CA1a cells (Starved) were treated with IGFBP7 before induction with insulin or IGF-1 and analyzed by immunoblotting. (**B**) Densitometric quantification of IGF1R and AKT phosphorylation from (A), normalized against the total amount of each corresponding protein. Corresponding values in IGF-1–induced cells in the absence of IGFBP7 were set as 1.0, and data are means ± SEM ($n = 3$ experiments, two-tailed Student's t test). (**C**) Serum-starved MCF10A cells were treated with IGFBP7 before induction with increasing concentrations of insulin, IGF-1, or IGF-2 and analyzed by immunoblotting. $n = 2$ experiments. (**D**) Immunoblot of proteins immunoprecipitated with IGF1Rβ or INSRβ antibodies from MCF10A cells pretreated with IGFBP7 and then left untreated or induced with insulin (80 ng/ml) or IGF-1 (50 ng/ml). $n = 2$ experiments.

IGFBP7 may affect the activity or abundance of plasma membrane–localized IGF1R. The IGF1R dynamics on the cell surface of serum-starved or IGF-1–treated MCF7 cells in response to IGFBP7 were analyzed by flow cytometry. High amounts of plasma membrane–localized IGF1R were detected in serum-starved cells, which were reduced from ~23 to 6% in response to IGF-1 stimulation (Fig. 2, A and B). This could be due to internalization of activated IGF1R (*1*). However, pretreatment of serum-starved cells with IGFBP7 resulted in substantial retention of plasma membrane–localized IGF1R, increasing its abundance more than twofold in IGF-1–stimulated cells, with the highest difference observed within 15 min of IGF-1 stimulation (Fig. 2B). These results are consistent with the notion that IGFBP7 directly or indirectly inhibits IGF-1 binding to IGF1R and subsequent internalization of the activated receptor by anchoring it in the plasma membrane. IGF-1 can likely overcome IGFBP7-mediated retention of IGF1R to an extent, based on the reduction of plasma membrane–localized IGF1R from ~36 to 13% in cells pretreated with IGFBP7 (Fig. 2, A and B).

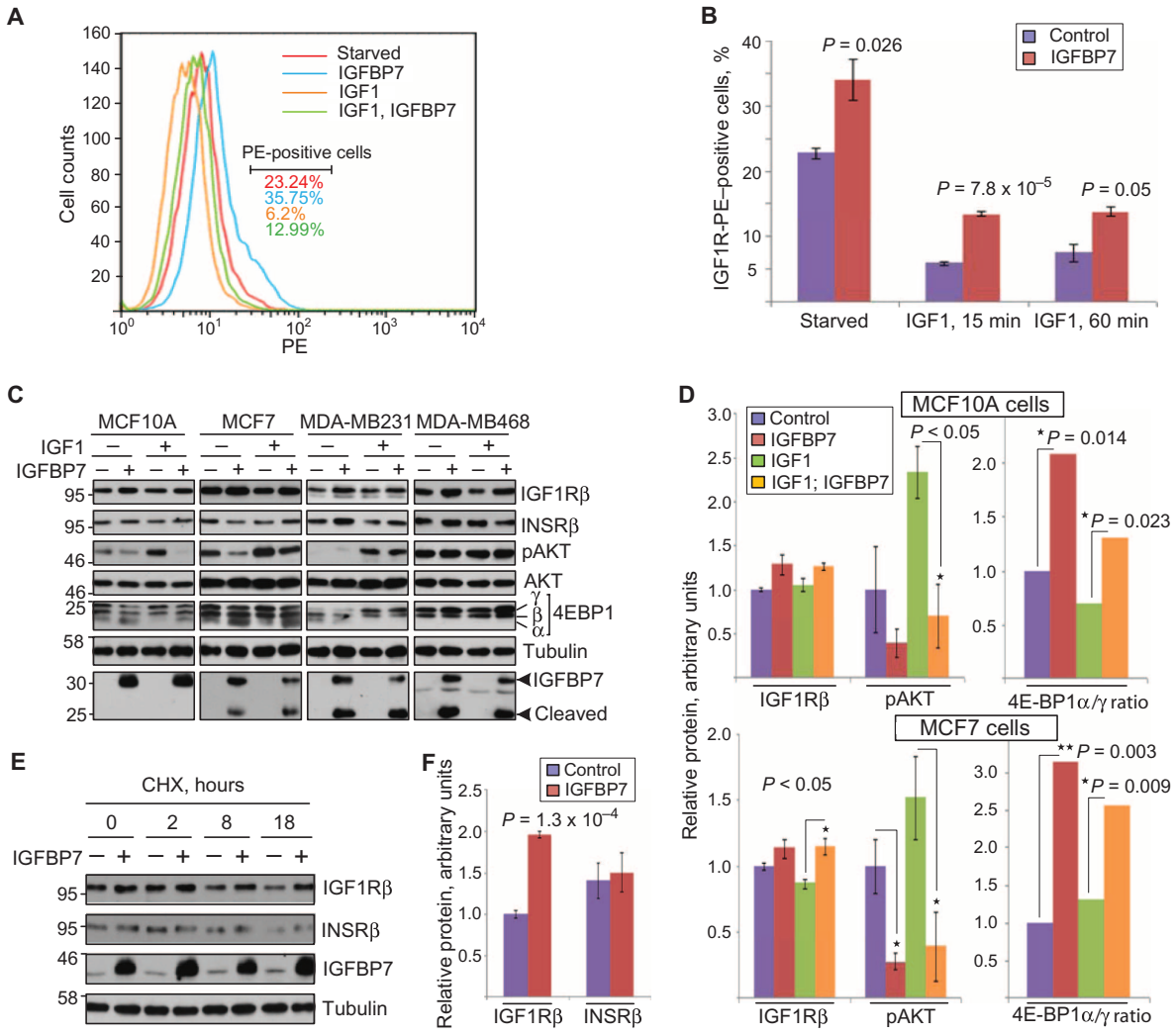

Fig. 2. IGFBP7 suppresses IGF1R internalization in response to IGF-1 and enhances IGF1Rβ protein stability. (**A**) Flow cytometric analysis of IGF1R-phycoerythrin (PE)–positive MCF7 cells treated with IGFBP7 before induction with IGF-1. (**B**) Data from three to six independent experiments as in (A) ± SEM are shown (two-tailed Student's *t* test). (**C**) Indicated cell lines were treated with IGFBP7 for 48 hours before induction with IGF-1 and analyzed by immunoblotting. (**D**) Densitometric quantification of IGF1Rβ and phosphorylated AKT in MCF10A and MCF7 cells from (C), normalized against tubulin or total AKT, respectively. Corresponding values in untreated control cells were set as 1.0, and data are means ± SEM (*n* = 3 experiments, two-tailed Student's *t* test). Panels to the right show the 4E-BP1α to 4E-BP1γ ratio calculated from (C) after normalization of the corresponding proteins to tubulin; *P* values were obtained by two-way analysis of variance (ANOVA) (*n* = 3 experiments). (**E**) MCF10A cells were treated with IGFBP7 before addition of cycloheximide (CHX) for the indicated times and analyzed by immunoblotting. (**F**) Densitometric quantification of IGF1Rβ and INSRβ after the 18-hour CHX treatment from (E), normalized against tubulin. Abundance of IGF1Rβ in untreated control cells was set as 1.0, and data are means ± SEM (*n* = 3 experiments, two-tailed Student's *t* test).

Given that internalization can lead to subsequent degradation of activated IGF1R (*1*), it was not surprising that the abundance of IGF1Rβ was somewhat increased in IGF-1–induced MCF7 cells after prolonged exposure to IGFBP7, whereas the abundance of INSRβ did not appear to be affected (Fig. 2, C and D). In line with its potential effect on IGF1R protein stability, IGF1Rβ, but not INSRβ, remained elevated in IGFBP7-treated MCF10A cells during 18 hours of treatment with cycloheximide (Fig. 2, E and F), a translational inhibitor used to assess protein stability (*27*). In addition to enhanced stability, prolonged exposure to IGFBP7 resulted in diminished responsiveness to IGF-1, as evidenced by reduced phosphorylation of AKT in MCF10A and MCF7 cells, where IGFBP7 was not substantially cleaved (Fig. 2, C and D).

As a potential downstream target molecule that might be affected in IGFBP7-treated cells, we tested 4E-binding protein 1 (4E-BP1), a translational repressor that, in its less phosphorylated α form, inhibits cap-dependent translation initiation by binding to the eukaryotic translation initiation factor eIF4E (*28*). Phosphorylation by mammalian target of rapamycin complex 1 (mTORC1), a kinase complex downstream of AKT, results in 4E-BP1 inactivation, thereby allowing eIF4E to activate protein synthesis (*28*). In agreement with other reports that show that 4E-BP1 is phosphorylated and inactivated in part through the AKT pathway (*29*), we found that phosphorylation of 4E-BP1 positively correlated with that of AKT in cell lines sensitive to IGF-1. For instance, in MCF10A and MCF7 cells, treatment with IGFBP7 resulted in reduced amounts of the slower-migrating highly phosphorylated 4E-BP1 γ form, whereas the faster-migrating, less phosphorylated α form was significantly increased (Fig. 2, C and D). By contrast, most 4E-BP1 was highly phosphorylated in MDA-MB231 cells (potentially because of substantial IGFBP7 cleavage) and in MDA-MB468 cells treated with IGFBP7 (Fig. 2C) or overexpressing IGFBP7 (fig. S2C), likely due to constitutively activated AKT. Therefore, in IGF-1–responsive cell lines, but not in those with aberrantly high PI3K-AKT signaling, IGFBP7 may promote translational repression by inhibiting the IGF1R-AKT-mTOR pathway and abrogating phosphorylation of 4E-BP1. In turn, this may lead to growth suppression and cell death because 4E-BP1 has been directly implicated in inducing apoptosis (*30*–*32*). Overall, these results demonstrate that IGFBP7 prevents activation of IGF1Rβ in response to IGF-1 and its subsequent internalization while enhancing the protein stability of IGF1Rβ.

Ectopic expression or treatment of xenograft tumors with IGFBP7 results in increased IGF1Rβ protein abundance

Increased abundance of IGF1R has been linked to less severe histopathological grade and improved breast cancer–specific survival in large cohorts of breast cancer patients, and phosphorylation, rather than total abundance, of IGF1R, has been suggested to be a better prognostic marker for responsiveness to IGF1R-targeting therapeutics (*33*–*35*). On the other hand, we have shown that xenograft tumors developed from IGFBP7-expressing MDA-MB468 cells or from MDA-MB231/1833 cells systemically treated with IGFBP7 exhibit reduced tumorigenicity and higher apoptotic rates (*36*, *37*). We therefore wondered if the observed reduced tumorigenicity could also be associated with increased abundance of IGF1R in these tumors. Indeed, immunohistochemistry revealed an increased IGF1Rβ signal in xenografts established from MDA-MB468 cells expressing IGFBP7 compared to those established from vector control cells (Fig. 3A). Moreover, IGF1Rβ abundance was increased in MDA-MB231/1833 xenografts when tumor-bearing mice were locally or intravenously injected with IGFBP7, and was also associated with IGFBP7 accumulation in tumor cells (Fig. 3B). Therefore, similar to its properties in cell lines, overexpression of or treatment with IGFBP7 appears to increase IGF1Rβ abundance in xenograft tumors. Together with the reported ability of IGFBP7 to inhibit proliferation in various cancer cell lines and tumor xenografts while inducing apoptosis (*36*, *37*), these results demonstrate that increased IGF1Rβ abundance in IGFBP7-treated tumors is not likely to be associated with enhanced IGF1R activity. Increased abundance of IGF1R may therefore serve as a marker for positive outcomes if IGFBP7 were to be used in clinical trials, as has been previously suggested (*37*, *38*).

IGFBP7 interacts with the extracellular portion of IGF1R in the absence of IGF-1

To gain further insight into the mechanism of IGFBP7-mediated IGF1R blockade, we used *Igf1r*-null mouse embryonic fibroblasts (MEFs) and their counterparts reconstituted with human IGF1R (*39*). We first tested whether IGFBP7 could interfere with receptor activation and downstream signaling in these cell lines. Because of the lack of IGF1R in *Igf1r*$^{-}$ MEFs, phosphorylation of IGF1Rβ was induced by IGF-1 exclusively in *IGF1R*$^{+}$ cells, was

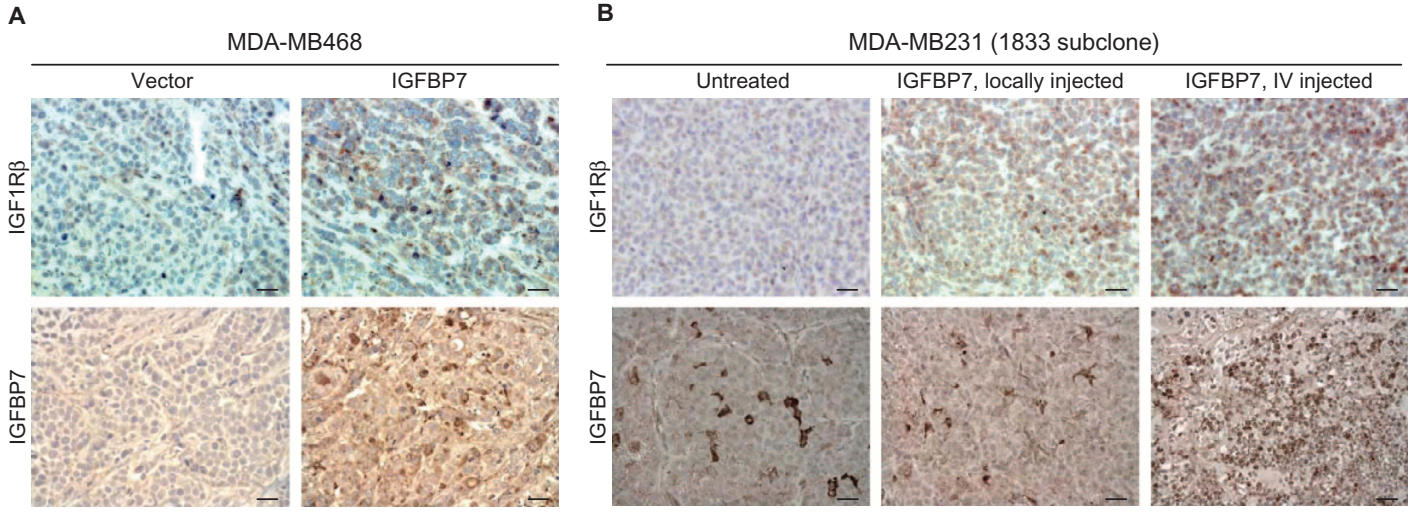

Fig. 3. Immunohistochemical staining showing increased IGF1Rβ abundance in xenograft tumors in response to IGFBP7 overexpression (**A**) or treatment (**B**). IV, intravenously. Scale bars, 25 μm. Images are representative of n = 4 xenografts per condition.

blocked by pretreatment with IGFBP7, and was associated with reduced phosphorylation of AKT (Fig. 4A). In contrast, insulin-induced phosphorylation of AKT did not appear to be affected in either cell line (Fig. 4A), further supporting the notion that IGFBP7 blocks IGF1R activation by IGF-1 but does not directly affect INSR activity.

To test whether IGFBP7 binds to IGF1R, we treated serum-starved cells with IGFBP7 and subjected them to immunoprecipitation. IGFBP7 coimmunoprecipitated with IGF1R but not with INSR (Fig. 4B). Analysis of *Igf1r*$^{-}$ MEFs that expressed a myristoylated plasma membrane–targeted form of the intracellular portion of IGF1Rβ (*40*) revealed, however, that IGFBP7 was unable to increase the abundance (Fig. 4C) or to coimmunoprecipitate with IGF1Rβ alone (Fig. 4D), suggesting that IGFBP7 is incapable of binding to or affecting the stability of the intracellular portion of IGF1R.

Given the ability of IGFBP7 to associate with the plasma membrane (fig. S3) and to reduce internalization of the plasma membrane–bound IGF1R in response to IGF-1 (Fig. 2, A and B), these results indicated that IGFBP7 may interact with IGF1R through its extracellular domain. To test this possibility, we treated serum-starved *Igf1r*$^{-}$ and *IGF1R*$^{+}$ MEFs with IGFBP7 in the presence or absence of IGF-1. Flow cytometry indicated that ~61% of IGFBP7-treated *IGF1R*$^{+}$ MEFs showed IGFBP7 binding, compared to less than 1% of *Igf1r*$^{-}$ cells (Fig. 4E, top panels), demonstrating that IGFBP7 can specifically bind to the extracellular portion of IGF1R. Moreover, the percentage of IGFBP7-positive *IGF1R*$^{+}$ cells was reduced by twofold in the presence of IGF-1 (Fig. 4E, bottom panels), substantiating the conclusion that IGFBP7 can bind to unoccupied IGF1R and that its interaction with IGF1R is reduced in the presence of IGF-1.

The N-terminal domain of IGFBP7 is required for interaction with IGF1R

To identify the IGFBP7 domain responsible for IGF1R binding, we tested a truncated recombinant IGFBP7 protein lacking the N-terminal 97 amino acids, which include the conserved cysteine-rich IGFBP motif shared by IGFBP1 to IGFBP6 and the heparin-binding site consisting of a cluster of basic amino acids that are important for interaction with cell-surface heparan sulfate proteoglycans (Fig. 5A) (*25*, *26*). The truncated form is generated in certain cancer cell lines by matriptase-mediated cleavage of full-length IGFBP7 between Lys^{97} and Ala^{98} (*41*). We found that IGFBP7 was more stable in *IGF1R*$^{+}$ MEFs (fig. S4A), suggesting that interaction with IGF1R may protect IGFBP7 against matriptase cleavage.

The truncated form did not inhibit IGF-1–induced phosphorylation of IGF1Rβ and AKT in *IGF1R*$^{+}$ cells (Fig. 5, B and C) or increase IGF1Rβ abundance during prolonged treatments (fig. S4A). Furthermore, full-length IGFBP7, but not the truncated form, reduced the accumulation of the highly phosphorylated γ form of 4E-BP1 in response to IGF-1 and

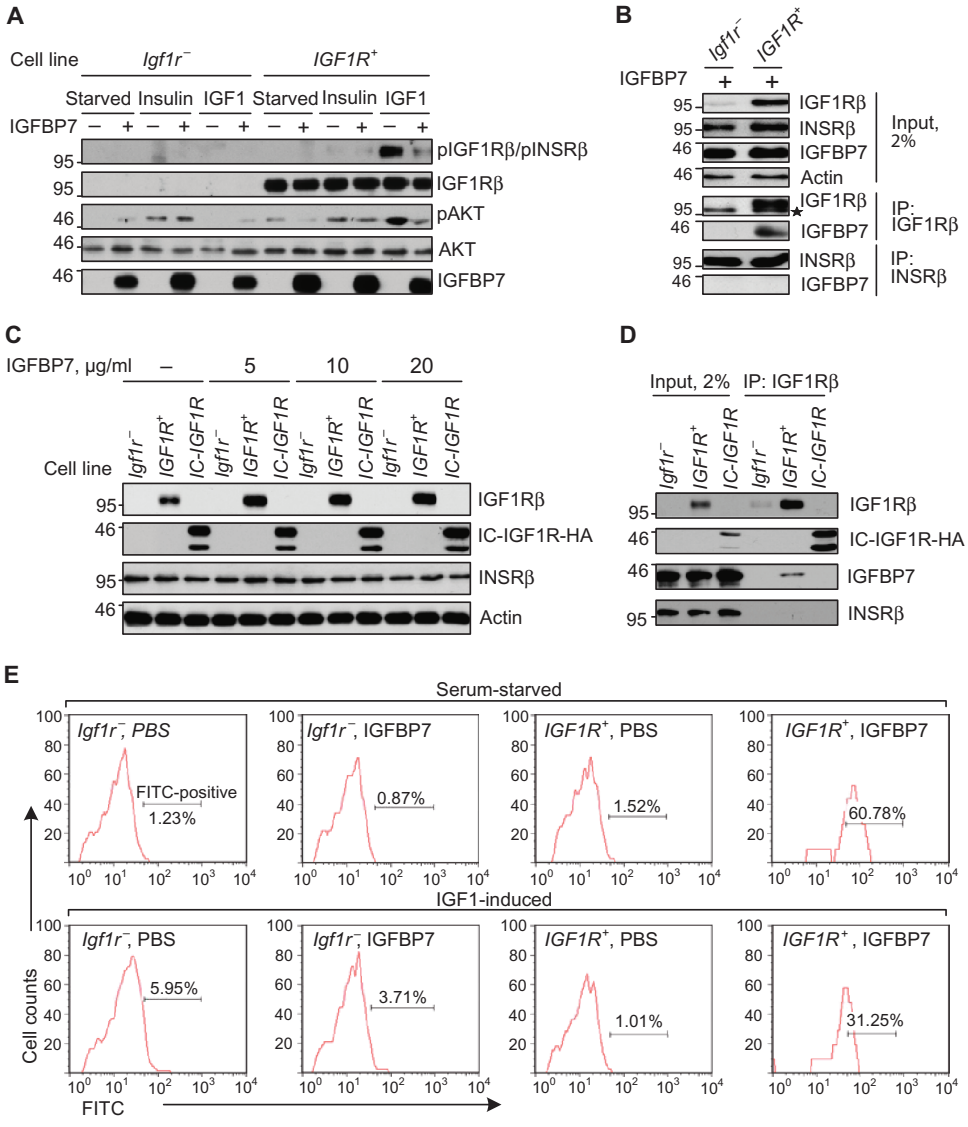

Fig. 4. IGFBP7 interacts with the extracellular portion of IGF1R in the absence of IGF-1. (**A**) Serum-starved MEFs were treated with IGFBP7 for 2 hours before induction with insulin or IGF-1 and analyzed by immunoblotting. (**B**) Immunoblot of proteins, as indicated, after immunoprecipitation with IGF1Rβ or INSRβ antibodies from serum-starved MEFs treated with IGFBP7 for 2 hours. The star indicates a cross-reacting protein. (**C**) *Igf1r*$^{-}$ MEFs expressing the myristoylated hemagglutinin (HA)–tagged intracellular (IC) portion of IGF1Rβ (IC-IGF1Rβ) along with control *Igf1r*$^{-}$ and *IGF1R*$^{+}$ cells were treated with the indicated concentrations of IGFBP7 for 24 hours and analyzed by immunoblotting. (**D**) Immunoblot of proteins, as indicated, after immunoprecipitation with IGF1Rβ antibodies from MEFs treated with IGFBP7 as in (B). (**E**) Flow cytometric analysis of IGFBP7 binding to *Igf1r*$^{-}$ and *IGF1R*$^{+}$ cells in the absence or presence of IGF-1. FITC, fluorescein isothiocyanate. The data shown in (A) to (E) are representative of three independent experiments.

increased the less phosphorylated α form of 4E-BP1 more than fourfold (Fig. 5, B and C). The failure of truncated IGFBP7 to suppress activation of the IGF1R–AKT–mTOR–4E-BP1 pathway despite its ability to penetrate both *Igf1r*$^{-}$ and *IGF1R*$^{+}$ cells (Fig. 5B and fig. S4A) may thus indicate that the extracellular IGFBP7-IGF1R interaction, and not cell penetration, could be important for this function. This was further confirmed by flow cytometry showing that the full-length IGFBP7 protein, but not the truncated form, bound to the surface of *IGF1R*$^{+}$ cells (Fig. 5D). Hence, the N-terminal 97–amino acid domain of IGFBP7 interacts with the extracellular portion of IGF1R and blocks its activity, and its loss abrogates the binding specificity of IGFBP7.

Full-length IGFBP7 induces apoptosis in an IGF1R-dependent manner

IGFBP7 inhibits tumor growth by inducing apoptosis or senescence (*11*, *12*, *37*). Indeed, we found that breast cancer cell lines treated with full-length IGFBP7 underwent apoptosis by day 4, as evidenced by increased amounts of poly(ADP-ribose) polymerase (PARP) and caspase 3 cleavage products (Fig. 6, A and B). In some cell lines, such as BT474 and MCF7, where a certain proportion of full-length IGFBP7 was still intact (Fig. 6A), we also detected variable amounts of the additional (smallest) 4E-BP1 form, which may represent the 4E-BP1 cleavage product that retains translation inhibitory activity (*42*). By contrast, in Hs578T cells, IGFBP7 had no effect on the abundance of apoptosis-associated molecules or phosphorylated AKT, likely because of lower IGF1R abundance and constitutive activation of AKT (Fig. 6, A and B).

Further analysis revealed that full-length IGFBP7 induced apoptosis in *IGF1R*$^{+}$ cells, as shown by increased cleavage of PARP and caspase 3 (Fig. 6C and fig. S4A). This was also associated with reduced AKT phosphorylation and higher IGF1Rβ abundance in these cells. Furthermore, consistent with competition between full-length IGFBP7 and IGF-1 for IGF1R binding, IGF-1, but not insulin, abrogated the proapoptotic activity of IGFBP7 in *IGF1R*$^{+}$ cells and diminished its ability to stabilize IGF1Rβ (fig. S4B), indicating that IGFBP7 exerts its effects mainly by interfering with the IGF1R-AKT pathway. In contrast, the truncated IGFBP7 protein did not affect IGF1Rβ abundance but weakly induced caspase 3 cleavage in both *Igf1r*$^{-}$ and *IGF1R*$^{+}$ cell lines (fig. S4A). Together with the observed lower but detectable cleavage of caspase 3 in *Igf1r*$^{-}$ cells treated with full-length IGFBP7 (Fig. 6C and fig. S4A), these results may indicate that the C-terminal IGFBP7 domain exhibits intrinsic proapoptotic activity that is not IGF1R-specific.

We also established that the enhanced susceptibility of *IGF1R*$^{+}$ cells to IGFBP7-driven apoptosis was not associated with changes in the abundance of BNIP3L (BCL2/adenovirus E1B 19 kD protein-interacting protein 3–like) protein (Fig. 6C), which acts downstream of IGFBP7 to induce apoptosis in B-RAF–transformed melanocytes (*43*). Likewise, the abundance of other Bcl-2 family members, including anti-apoptotic Bcl-2 and proapoptotic Bad and Bax, was not affected in an IGFBP7-dependent manner (Fig. 6C), arguing against the possibility that changes in their abundance could contribute to IGFBP7-induced apoptosis.

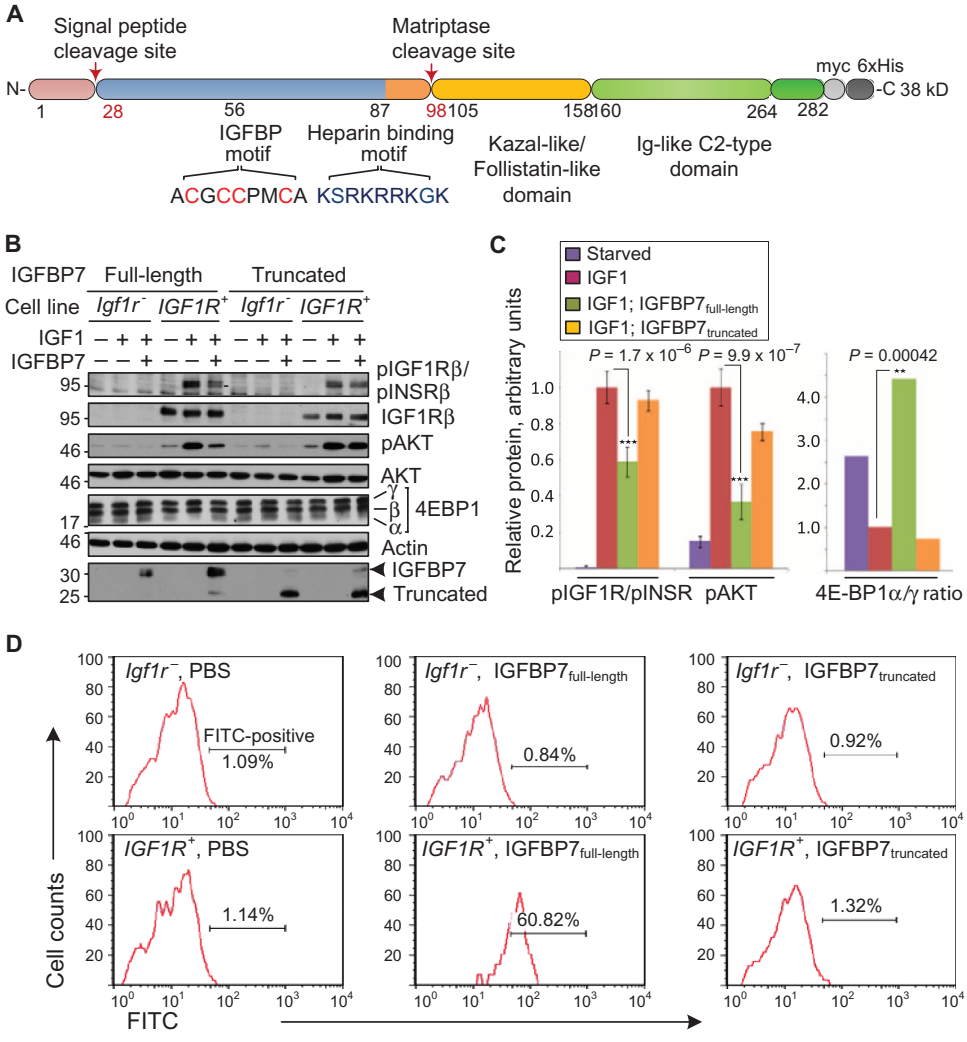

Fig. 5. The N-terminal IGFBP7 domain is required for interaction with IGF1R. (**A**) Domain organization of IGFBP7 with indicated cleavage sites and c-myc and histidine (His) tags. (**B**) Serum-starved MEFs were treated with recombinant full-length or truncated IGFBP7 proteins before induction with IGF-1 and analyzed by immunoblotting. (**C**) Densitometric quantification of phosphorylated forms of IGF1Rβ and AKT in *IGF1R*$^{+}$ MEFs from (B), normalized against the total amount of each corresponding protein. Corresponding values in IGF-1–induced cells in the absence of IGFBP7 were set as 1.0, and data are means ± SEM (n = 3 experiments, two-tailed Student's t test). Panels to the right show the 4E-BP1α to 4E-BP1γ ratio calculated from (B) after normalization of corresponding proteins to actin; P values were obtained by two-way ANOVA (n = 3 experiments). (**D**) Binding of full-length or truncated IGFBP7 proteins to *Igf1r*$^{-}$ and *IGF1R*$^{+}$ cells was analyzed by flow cytometry. Representative results from two independent experiments are shown.

To further elucidate whether specific blockade of the IGF1R-AKT pathway is sufficient to sensitize *IGF1R*$^+$ cells to apoptosis, we used BMS-536924, an adenosine 5′-triphosphate competitor that blocks both IGF1R and INSR (*44*), and picropodophyllin (PPP) an IGF1R inhibitor that prevents phosphorylation of Tyr^{1136} in the kinase activation loop (*45*). Using *Igf1r*$^-$ and *IGF1R*$^+$ cell lines, we found that pretreatment with BMS-536924 or PPP significantly inhibited IGF-1–induced phosphorylation of IGF1R and AKT in *IGF1R*$^+$ cells (Fig. 6, D and E). Prolonged treatment with these drugs induced apoptosis, as judged by the increased cleavage of caspase 3 and PARP (Fig. 6F). With the highest inhibitor doses, the abundance of cleaved forms of caspase 3 and PARP in *IGF1R*$^+$ cells was increased more than sixfold and was comparable to that caused by IGFBP7 (Fig. 6G). Furthermore, IGF1Rβ abundance was significantly increased in IGFBP7-treated *IGF1R*$^+$ cells but not in drug-treated cells (Fig. 6, F and G), indicating that IGF1Rβ stabilization cannot be achieved by simple inhibition of IGF1R activity. Therefore, IGFBP7 may safeguard IGF1R integrity and prevent inappropriate activation (Fig. 7).

DISCUSSION

This study demonstrates that IGFBP7 acts as an IGF-1/2 antagonist that can block IGF1R activation by binding to the receptor itself. This is in contrast to IGFBP1 to IGFBP6, which sequester IGF-1 and IGF-2 into inactive complexes (*10*). The IGF1R inhibitory activity exhibited by

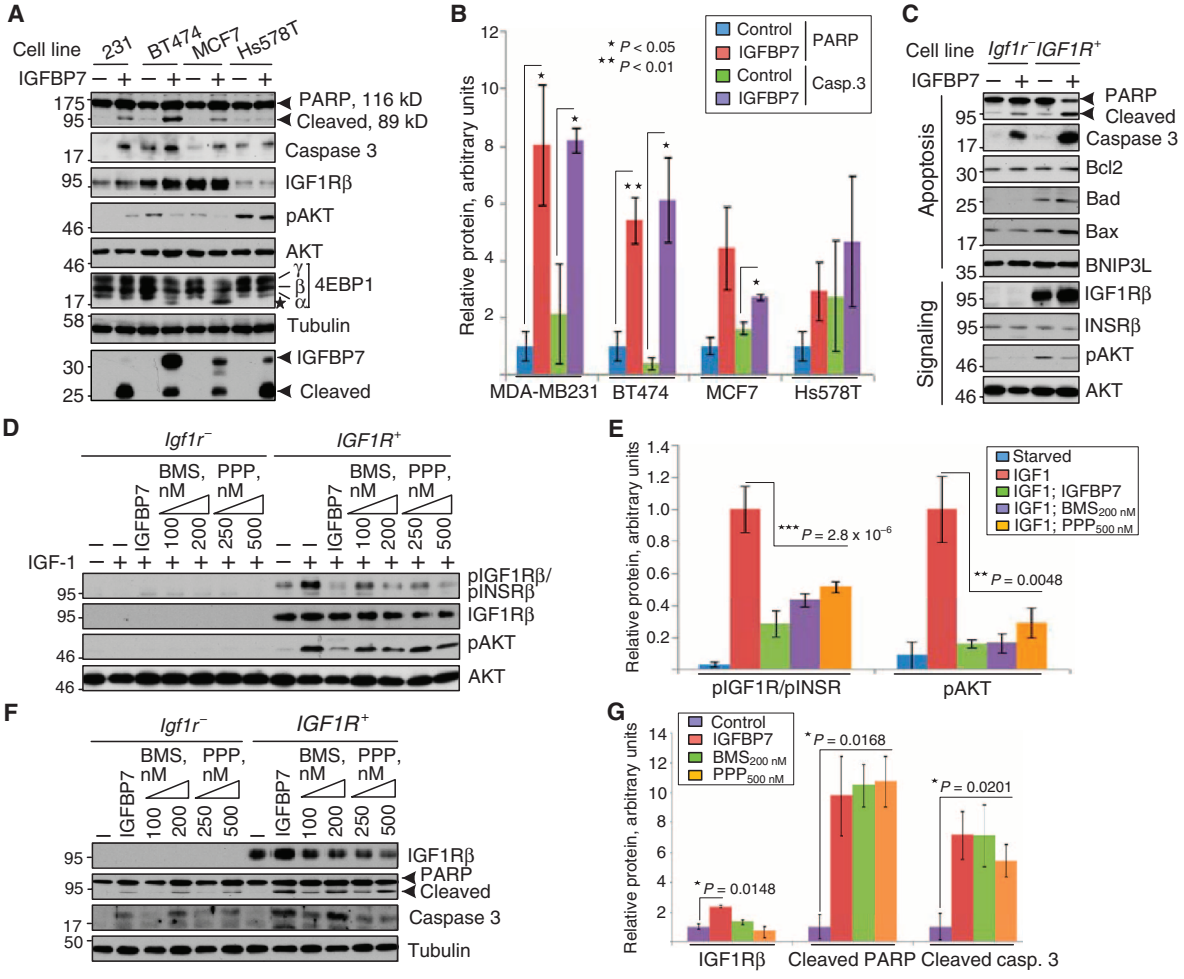

Fig. 6. Full-length IGFBP7 induces apoptosis in an IGF1R-dependent manner. (**A**) Breast cancer cell lines were treated with IGFBP7 for 4 days and analyzed by immunoblotting. The star indicates the 4E-BP1 cleavage product. (**B**) Densitometric quantification of cleaved forms of PARP and caspase 3 from (A), normalized against total tubulin. Corresponding values in untreated control cells were set as 1.0, and data are means ± SEM (*n* = 3 experiments, two-tailed Student's *t* test). (**C**) MEFs were treated with IGFBP7 for 3 days and analyzed by immunoblotting. (**D**) Serum-starved MEFs were treated for 1 hour with IGFBP7, BMS-536924, or PPP before induction with IGF-1 for 5 min. (**E**) Densitometric quantification of IGF1R and AKT phosphorylation in *IGF1R*$^+$ cells from (D), normalized against the total amount of each corresponding protein. Corresponding values of IGF-1–induced phosphorylation in the absence of IGFBP7 were set as 1.0, and data are means ± SEM (*n* = 3 experiments, one-way ANOVA). (**F**) MEFs were treated with IGFBP7, BMS-536924, or PPP for 2 days and analyzed by immunoblotting. (**G**) Densitometric quantification of IGF1Rβ and cleaved forms of PARP and caspase 3 in *IGF1R*$^+$ cells from (F), normalized against tubulin. Corresponding values in untreated control cells were set as 1.0, and data are means ± SEM (*n* = 3 experiments, one-way ANOVA).

IGFBP7 is comparable to that of specific IGF1R-targeting drugs such as BMS-536924 and PPP, including reduced phosphorylation of AKT and induction of apoptosis during prolonged treatments. Our findings indicate that the IGF1R–AKT–mTOR–4E-BP1 axis is a major IGFBP7 target, which, when inhibited, leads to apoptosis (Fig. 7). Another unexpected finding of this study is that IGFBP7-mediated blockade of IGF1R activity was accompanied by enhanced IGF1Rβ stability. We discovered a mechanism whereby IGFBP7 anchors inactive IGF1R on the cell surface and prevents its internalization in response to IGF-1, which, in turn, may result in IGF1Rβ stabilization. Increased IGF1Rβ protein abundance was observed not only in cell lines but also in xenograft tumors treated with IGFBP7, where it was also associated with reduced tumorigenicity and more pronounced apoptosis (*36*, *37*). Our observations are consistent with the finding that an increase in abundance of the phosphorylated (activated) form of IGF1R, and not that of total IGF1R, is a stronger indicator of poor prognosis (*33*–*35*). We thus propose that IGFBP7 is a component of the physiological mechanism directed to preserve IGF1R integrity during differentiation or maintenance of normal tissues while restricting uncontrolled proliferative and prosurvival signaling. Increased abundance of total IGF1R in tumors may thus indicate a more differentiated and less malignant phenotype that potentially involves IGFBP7. In contrast, decreased IGFBP7 abundance observed in advanced cancers (*12*) may lead to increased activation of the IGF1R pathway, contributing to metastatic progression.

We determined that the N-terminal 97 amino acids of IGFBP7 are critically important for the interaction with the extracellular portion of IGF1R and that their deletion abolishes the ability of IGFBP7 to specifically bind to IGF1R and inhibit its activation. In this regard, the ability of matriptase to cleave these critical 97 amino acids suggests a cellular mechanism that could overcome the IGF1R-dependent inhibitory activity of IGFBP7. As established in this study, other strategies developed by cancer cells to escape the proapoptotic effects of IGFBP7 include decreased abundance of IGFBP7 or IGF1R, constitutive activation of AKT signaling due to *RAS* or *PTEN* mutations, or *EGFR* or *HER2* amplification (Fig. 7). Activation of these and other pathways [such as platelet-derived growth factor receptor (*7*)] have been reported to increase PI3K-AKT-mTOR signaling and to limit the efficacy of specific IGF1R and AKT inhibitors in mouse models and clinical trials (*5*, *8*, *32*).

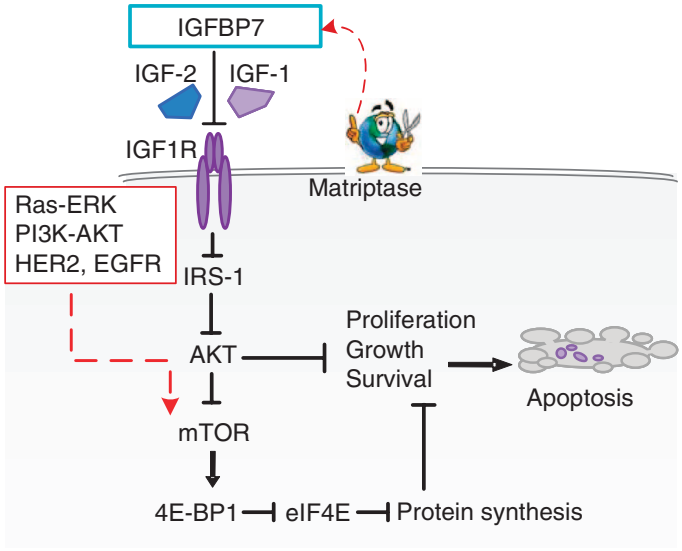

Fig. 7. Proposed model for IGFBP7-mediated regulation of IGF1R activity. IGFBP7 binds to the extracellular portion of IGF1R in the absence of IGF-1/2 through its N-terminal 97–amino acid domain, thereby blocking IRS-1 phosphorylation and downstream PI3K–AKT–mTOR–4E-BP1 signaling. This, in turn, results in inhibition of protein synthesis, suppression of cell growth and proliferation, and, eventually, activation of apoptosis in an IGF1R-dependent manner. The inhibitory effects of IGFBP7 can be reversed by (i) IGF-1 or IGF-2 because they have higher affinity to IGF1R; (ii) activating mutations in the PI3K-AKT, Ras-ERK, EGFR, or other pathways converging downstream of IGF1R; or (iii) plasma membrane–bound matriptase, which cleaves the N-terminal IGF1R-binding domain.

Several lines of evidence indicate that the binding of IGFBP7 and that of IGF-1 to IGF1R are mutually exclusive, and that IGFBP7 binds in the absence of IGF-1. First, IGFBP7 coimmunoprecipitated with IGF1R and bound to a greater extent to the surface of *IGF1R*$^+$ cells in serum- and IGF-1–deprived cells than in cells treated with IGF-1. Furthermore, IGFBP7-mediated retention of IGF1R on the plasma membrane was reduced in response to IGF-1. Second, independent of the cell type, IGFBP7 required preincubation with cells to block subsequent IGF-1–mediated IGF1R activation. IGFBP7 preincubation with IGF-1 or their simultaneous addition to the cells did not prevent IGF-1–induced IGF1R phosphorylation or activation of downstream signaling, suggesting that IGFBP7 cannot directly compete with IGF-1 for IGF1R binding and is a weaker IGF1R binding partner. These results support the notion that IGFBP7 binds to unligated IGF1R and occupies the same or adjacent binding site, thereby sterically restricting binding of IGF-1 or causing conformational changes in the receptor that prevent IGF-1 from binding.

Similar to IGFBP7, IGFBP3, but not IGFBP1 or IGFBP5, has also been reported to compete with an IGF-1 analog for binding to the cell surface and to block IGF1R activation, although a potential mechanism did not appear to involve its direct interaction with IGF1R (*46*, *47*). Furthermore, the N-terminal 95–amino acid IGFBP3 domain, which shows ~30% similarity to that of IGFBP7, interferes with the mitogenic actions of IGF-1, despite the lack of IGF-1–binding ability (*48*). It is thus conceivable that in addition to its ability to sequester IGF-1, IGFBP3 may also directly suppress IGF1R activation through its N-terminal domain, paralleling the effects we have observed for IGFBP7.

Boucher *et al.* have described IGF1R and INSR as dependence receptors that induce antiapoptotic signals in the presence of the ligand and proapoptotic signals in the absence of the ligand (*49*). In this regard, IGFBP7 could be viewed as a missing link in the dependence receptor model, which, upon binding to unoccupied IGF1R, induces its intrinsic proapoptotic activity. However, we favor the possibility that IGFBP7 triggers apoptosis by suppressing IGF1R-AKT-mTOR signaling in IGF-1–sensitive cells, including MCF10A and MCF7 cells and *IGF1R*$^+$ MEFs tested in this study. In contrast to the brown preadipocyte cell models used by Boucher *et al.* in which either IGF1R or INSR can induce apoptosis, in our normal and breast cancer cell lines, IGFBP7 exerted its proapoptotic effects primarily through IGF1R. Furthermore, we found that IGF1R blockade by IGFBP7 did not affect or, in some cell lines including MDA-MB468-IGFBP7 cells, even induced INSR activity and insulin sensitivity, in accord with other reports showing that INSR may substitute for the loss of IGF1R (*2*, *5*, *8*, *9*, *23*, *24*). It thus cannot be excluded that cancers with increased INSR abundance may be less responsive to IGFBP7 treatments because of a compensatory response.

In summary, we provide evidence here that IGFBP7 elicits its effects through direct targeting of unoccupied IGF1R, leading to its increased abundance and decreased activity and enhanced propensity of IGF1R-positive cells to apoptosis. These findings suggest that IGFBP7 could have substantial

clinical efficacy in IGF1R-driven tumors while having minimal, if any, effects on normal tissues.

MATERIALS AND METHODS

IGFBP7 cloning and purification

The complementary DNA coding for the human full-length IGFBP7 protein was cloned into Bam HI–Xho I sites of the pSec-tag2B secretion signal bearing vector (Invitrogen), as previously described (*36*). Truncated IGFBP7 was generated from the same construct by introducing Bam HI site just proximal to the matriptase cleavage site. Digestion of this construct with Bam HI yielded a plasmid coding for the truncated His- and c-myc–tagged IGFBP7 protein lacking the N-terminal 97 amino acids. Purification of the full-length and truncated IGFBP7 proteins was done with His-Select Nickel Affinity gel (Sigma) from the conditioned medium collected from the stably transfected MDA-MB468 cells grown in Opti-MEM medium containing 2% fetal bovine serum (FBS), as previously described (*36*, *37*).

Cell cultures and treatments

Breast cancer cell lines were obtained from the American Type Culture Collection and maintained in regular Dulbecco's modified Eagle's medium (DMEM) (Gibco) supplemented with 10% FBS. MCF10A and MCF10CA1a cells were cultured in medium containing 5% horse serum, as previously described (*17*). *Igf1r*$^{-}$ and *IGF1R*$^{+}$ MEFs were cultured in low-glucose DMEM (1 g/liter; Gibco) supplemented with 10% FBS. Serum-starved cells were treated with the recombinant full-length or truncated IGFBP7 proteins (20 μg/ml of each) for 2 hours in serum-free medium followed by induction with insulin (10 μg/ml) or IGF-1 (50 ng/ml) for 15 min, unless stated otherwise. Where indicated, cells were treated with BMS-536924 (provided to M.P. by Bristol Myers Squibb through a material transfer agreement) and PPP (Calbiochem).

Immunoblotting and immunoprecipitation

Cell lysis, fractionation, and immunoprecipitation were done as previously described (*50*). Immunoblotting was performed with the following antibodies from Cell Signaling: pAKT (Ser^{473}; 4058), total AKT (9272), pERK1/2 (4377), ERK1/2 (4695), PARP (9542), cleaved caspase 3 (Asp^{175}; 9661), pIGF1Rβ/INSRβ (3021), 4E-BP1 (9452), Bax (2772), Bcl-2 (2876), and Bad (9292). Other antibodies used in this study were c-myc (sc-40), IRS-1 (sc-559), IGF1Rβ (sc-713), and INSRβ (sc-57342), purchased from Santa Cruz Biotechnology; tubulin (T5293, Sigma); HA (MMS-101P; Covance); BNIP3L (2289; ProScience Inc.); and actin (a custom-made antibody).

Previous reports have normalized cleaved PARP to the loading controls and presented immunoblots of cleaved caspase 3 without also showing uncleaved caspase 3 (*51*–*54*).

The ratio of 4E-BP1α to 4E-BP1γ was quantified and presented without error bars as has been previously done for other proteins (*55*, *56*). The SE could not be properly estimated for the ratios without making additional assumptions about the data.

Xenografting and immunohistochemistry

Xenografts were developed from MDA-MB468 cells ectopically expressing IGFBP7 or vector alone or from a highly malignant MDA-MB231/1833 subclone injected into the flanks of nonobese diabetic–severe combined immunodeficient mice. Treatment of 1833 tumors with IGFBP7 was done by local or intravenous injections every 4 days until the end point of the experiment (day 26), as previously described (*39*). Immunohistochemistry on formalin-fixed paraffin-embedded tissues was performed as described (*36*), using IGF1Rβ (1:20) or IGFBP7 (1:150; sc-6064, Santa Cruz Biotechnology) antibodies and the OmniMap-HRP Kit (Ventana) and hematoxylin and eosin for counterstaining. Staining was done with the Ventana Discovery instrument (Ventana). Images were acquired with an Axioplan2 microscope (Zeiss) and converted to TIFF format.

Flow cytometry

For IGFBP7 binding studies, serum-starved MEFs seeded in six-well plates (~1 × 10^{6} per well) were treated with full-length or truncated IGFBP7s (20 μg/ml) in the absence or presence of IGF-1 (50 ng/ml) for 4 hours. Cells were scraped out without trypsinization, washed with phosphate-buffered saline (PBS), and incubated with primary IGFBP7 antibodies diluted 1:500 in 0.5% bovine serum albumin (BSA)–PBS for 30 min at 4°C. After being washed with the same buffer, cells were incubated with secondary anti-rabbit-FITC antibodies (Sigma) for 30 min at 4°C, washed twice, and resuspended in PBS containing 0.5% BSA and propidium iodide (PI; Invitrogen; 1 μg/ml) or 7-amino-actinomycin D (7-AAD; BioLegend; 5 μg/ml), for dead cell exclusion. Plasma membrane–bound IGF1R was detected in MCF7 cells (250,000 per well in six-well plates) treated overnight with IGFBP7 (40 μg/ml) or PBS in serum-free low-glucose DMEM, followed by induction with IGF-1 (50 ng/ml) for 15 or 60 min. Cells were collected by trypsinization, washed, and incubated with PE-labeled IGF1R antibodies (MCA2344PET, AbD Serotec). Samples were analyzed with a FACSCalibur flow cytometer (Becton Dickinson) with the CellQuest Pro software (BD Biosciences). Gating was set to control cells stained with 7-AAD or PI as indicated.

Statistical analysis

To ensure the applicability of standard analysis techniques, we first confirmed that the data were normally distributed by means of histograms and Q-Q plots. *F*-tests were used to ensure that the proteins used for normalization had significantly lower variance than the proteins being tested, allowing us to take ratios to normalize the data. Normalized data were compared with unadjusted two-tailed Student's *t* tests or one- or two-way ANOVA, where appropriate, for two or multiple variables, using SPSS 20 software and Microsoft Excel.

SUPPLEMENTARY MATERIALS

www.sciencesignaling.org/cgi/content/full/5/255/ra92/DC1

Fig. S1. IGFBP7 does not interfere with activation of the IGF1R or INSR pathways when added simultaneously with their cognate ligands.

Fig. S2. Pretreatment with IGFBP7 or its ectopic expression in cancer cell lines inhibits IGF-1–mediated activation of IGF1R.

Fig. S3. Plasma membrane localization of IGFBP7 in treated or transfected cell lines.

Fig. S4. Full-length but not the truncated form of IGFBP7 induces apoptosis in the absence of IGF-1.

REFERENCES AND NOTES

1. A. A. Samani, S. Yakar, D. LeRoith, P. Brodt, The role of the IGF system in cancer growth and metastasis: Overview and recent insights. *Endocr. Rev.* **28**, 20–47 (2007).
2. F. Frasca, G. Pandini, L. Sciacca, V. Pezzino, S. Squatrito, A. Belfiore, R. Vigneri, The role of insulin receptors and IGF-I receptors in cancer and other diseases. *Arch. Physiol. Biochem.* **114**, 23–37 (2008).
3. S. A. Rosenzweig, H. S. Atreya, Defining the pathway to insulin-like growth factor system targeting in cancer. *Biochem. Pharmacol.* **80**, 1115–1124 (2010).
4. M. Pollak, Insulin and insulin-like growth factor signalling in neoplasia. *Nat. Rev. Cancer* **8**, 915–928 (2008).
5. M. Pollak, The insulin and insulin-like growth factor receptor family in neoplasia: An update. *Nat. Rev. Cancer* **12**, 159–169 (2012).
6. J. C. Potratz, D. N. Saunders, D. H. Wai, T. L. Ng, S. E. McKinney, J. M. Carboni, M. M. Gottardis, T. J. Triche, H. Jürgens, M. N. Pollak, S. A. Aparicio, P. H. Sorensen,

Synthetic lethality screens reveal RPS6 and MST1R as modifiers of insulin-like growth factor-1 receptor inhibitor activity in childhood sarcomas. *Cancer Res.* **70**, 8770–8781 (2010).
7. C. I. Campbell, R. A. Moorehead, Mammary tumors that become independent of the type I insulin-like growth factor receptor express elevated levels of platelet-derived growth factor receptors. *BMC Cancer* **11**, 480 (2011).
8. E. Buck, M. Mulvihill, Small molecule inhibitors of the IGF-1R/IR axis for the treatment of cancer. *Expert Opin. Investig. Drugs* **20**, 605–621 (2011).
9. A. Belfiore, F. Frasca, G. Pandini, L. Sciacca, R. Vigneri, Insulin receptor isoforms and insulin receptor/insulin-like growth factor receptor hybrids in physiology and disease. *Endocr. Rev.* **30**, 586–623 (2009).
10. S. M. Firth, R. C. Baxter, Cellular actions of the insulin-like growth factor binding proteins. *Endocr. Rev.* **23**, 824–854 (2002).
11. V. Hwa, Y. Oh, R. G. Rosenfeld, The insulin-like growth factor-binding protein (IGFBP) superfamily. *Endocr. Rev.* **20**, 761–787 (1999).
12. A. M. Burger, B. Leyland-Jones, K. Banerjee, D. D. Spyropoulos, A. K. Seth, Essential roles of IGFBP-3 and IGFBP-rP1 in breast cancer. *Eur. J. Cancer* **41**, 1515–1527 (2005).
13. Y. Oh, S. R. Nagalla, Y. Yamanaka, H. S. Kim, E. Wilson, R. G. Rosenfeld, Synthesis and characterization of insulin-like growth factor-binding protein (IGFBP)-7. Recombinant human mac25 protein specifically binds IGF-I and -II. *J. Biol. Chem.* **271**, 30322–30325 (1996).
14. K. Akaogi, J. Sato, Y. Okabe, Y. Sakamoto, H. Yasumitsu, K. Miyazaki, Synergistic growth stimulation of mouse fibroblasts by tumor-derived adhesion factor with insulin-like growth factors and insulin. *Cell Growth Differ.* **7**, 1671–1677 (1996).
15. Y. Yamanaka, E. M. Wilson, R. G. Rosenfeld, Y. Oh, Inhibition of insulin receptor activation by insulin-like growth factor binding proteins. *J. Biol. Chem.* **272**, 30729–30734 (1997).
16. Y. Sato, Z. Chen, K. Miyazaki, Strong suppression of tumor growth by insulin-like growth factor-binding protein-related protein 1/tumor-derived cell adhesion factor/mac25. *Cancer Sci.* **98**, 1055–1063 (2007).
17. S. J. Santner, P. J. Dawson, L. Tait, H. D. Soule, J. Eliason, A. N. Mohamed, S. R. Wolman, G. H. Heppner, F. R. Miller, Malignant MCF10CA1 cell lines derived from premalignant human breast epithelial MCF10AT cells. *Breast Cancer Res. Treat.* **65**, 101–110 (2001).
18. D. Yee, G. S. Lebovic, R. R. Marcus, N. Rosen, Identification of an alternate type I insulin-like growth factor receptor β subunit mRNA transcript. *J. Biol. Chem.* **264**, 21439–21441 (1989).
19. A. Hollestelle, F. Elstrodt, J. H. Nagel, W. W. Kallemeijn, M. Schutte, Phosphatidylinositol-3-OH kinase or RAS pathway mutations in human breast cancer cell lines. *Mol. Cancer Res.* **5**, 195–201 (2007).
20. G. M. Yanochko, W. Eckhart, Type I insulin-like growth factor receptor over-expression induces proliferation and anti-apoptotic signaling in a three-dimensional culture model of breast epithelial cells. *Breast Cancer Res.* **8**, R18 (2006).
21. C. E. Tognon, A. M. Somasiri, V. E. Evdokimova, G. Trigo, E. E. Uy, N. Melnyk, J. M. Carboni, M. M. Gottardis, C. D. Roskelley, M. Pollak, P. H. Sorensen, ETV6-NTRK3–mediated breast epithelial cell transformation is blocked by targeting the IGF1R signaling pathway. *Cancer Res.* **71**, 1060–1070 (2011).
22. D. K. Armstrong, S. H. Kaufmann, Y. L. Ottaviano, Y. Furuya, J. A. Buckley, J. T. Isaacs, N. E. Davidson, Epidermal growth factor-mediated apoptosis of MDA-MB-468 human breast cancer cells. *Cancer Res.* **54**, 5280–5283 (1994).
23. H. Zhang, A. M. Pelzer, D. T. Kiang, D. Yee, Down-regulation of type I insulin-like growth factor receptor increases sensitivity of breast cancer cells to insulin. *Cancer Res.* **67**, 391–397 (2007).
24. E. Buck, P. C. Gokhale, S. Koujak, E. Brown, A. Eyzaguirre, N. Tao, M. Rosenfeld-Franklin, L. Lerner, M. I. Chiu, R. Wild, D. Epstein, J. A. Pachter, M. R. Miglarese, Compensatory insulin receptor (IR) activation on inhibition of insulin-like growth factor-1 receptor (IGF-1R): Rationale for cotargeting IGF-1R and IR in cancer. *Mol. Cancer Ther.* **9**, 2652–2664 (2010).
25. J. Sato, S. Hasegawa, K. Akaogi, H. Yasumitsu, S. Yamada, K. Sugahara, K. Miyazaki, Identification of cell-binding site of angiomodulin (AGM/TAF/Mac25) that interacts with heparan sulfates on cell surface. *J. Cell. Biochem.* **75**, 187–195 (1999).
26. J. Kishibe, S. Yamada, Y. Okada, J. Sato, A. Ito, K. Miyazaki, K. Sugahara, Structural requirements of heparan sulfate for the binding to the tumor-derived adhesion factor/angiomodulin that induces cord-like structures to ECV-304 human carcinoma cells. *J. Biol. Chem.* **275**, 15321–15329 (2000).
27. P. Zhou, Determining protein half-lives. *Methods Mol. Biol.* **284**, 67–77 (2004).
28. A. C. Gingras, B. Raught, N. Sonenberg, eIF4 initiation factors: Effectors of mRNA recruitment to ribosomes and regulators of translation. *Annu. Rev. Biochem.* **68**, 913–963 (1999).
29. A. C. Gingras, S. G. Kennedy, M. A. O'Leary, N. Sonenberg, N. Hay, 4E-BP1, a repressor of mRNA translation, is phosphorylated and inactivated by the Akt(PKB) signaling pathway. *Genes Dev.* **12**, 502–513 (1998).
30. S. Li, N. Sonenberg, A. C. Gingras, M. Peterson, S. Avdulov, V. A. Polunovsky, P. B. Bitterman, Translational control of cell fate: Availability of phosphorylation sites on translational repressor 4E-BP1 governs its proapoptotic potency. *Mol. Cell. Biol.* **22**, 2853–2861 (2002).
31. B. A. Jacobson, M. D. Alter, M. G. Kratzke, S. P. Frizelle, Y. Zhang, M. S. Peterson, S. Avdulov, R. P. Mohorn, B. A. Whitson, P. B. Bitterman, V. A. Polunovsky, R. A. Kratzke, Repression of cap-dependent translation attenuates the transformed phenotype in non–small cell lung cancer both in vitro and in vivo. *Cancer Res.* **66**, 4256–4262 (2006).
32. Q. B. She, E. Halilovic, Q. Ye, W. Zhen, S. Shirasawa, T. Sasazuki, D. B. Solit, N. Rosen, 4E-BP1 is a key effector of the oncogenic activation of the AKT and ERK signaling pathways that integrates their function in tumors. *Cancer Cell* **18**, 39–51 (2010).
33. J. H. Law, G. Habibi, K. Hu, H. Masoudi, M. Y. Wang, A. L. Stratford, E. Park, J. M. Gee, P. Finlay, H. E. Jones, R. I. Nicholson, J. Carboni, M. Gottardis, M. Pollak, S. E. Dunn, Phosphorylated insulin-like growth factor-I/insulin receptor is present in all breast cancer subtypes and is related to poor survival. *Cancer Res.* **68**, 10238–10246 (2008).
34. R. Yerushalmi, K. A. Gelmon, S. Leung, D. Gao, M. Cheang, M. Pollak, G. Turashvili, B. C. Gilks, H. Kennecke, Insulin-like growth factor receptor (IGF-1R) in breast cancer subtypes. *Breast Cancer Res. Treat.* **132**, 131–142 (2012).
35. P. Fu, M. Ibusuki, Y. Yamamoto, M. Hayashi, K. Murakami, S. Zheng, H. Iwase, Insulin-like growth factor-1 receptor gene expression is associated with survival in breast cancer: A comprehensive analysis of gene copy number, mRNA and protein expression. *Breast Cancer Res. Treat.* **130**, 307–317 (2011).
36. Y. Amemiya, W. Yang, T. Benatar, S. Nofech-Mozes, A. Yee, H. Kahn, C. Holloway, A. Seth, Insulin like growth factor binding protein-7 reduces growth of human breast cancer cells and xenografted tumors. *Breast Cancer Res. Treat.* **126**, 373–384 (2011).
37. T. Benatar, W. Yang, Y. Amemiya, V. Evdokimova, H. Kahn, C. Holloway, A. Seth, IGFBP7 reduces breast tumor growth by induction of senescence and apoptosis pathways. *Breast Cancer Res. Treat.* **133**, 563–573 (2012).
38. N. Wajapeyee, V. Kapoor, M. Mahalingam, M. R. Green, Efficacy of IGFBP7 for treatment of metastatic melanoma and other cancers in mouse models and human cell lines. *Mol. Cancer Ther.* **8**, 3009–3014 (2009).
39. C. Sell, G. Dumenil, C. Deveaud, M. Miura, D. Coppola, T. DeAngelis, R. Rubin, A. Efstratiadis, R. Baserga, Effect of a null mutation of the insulin-like growth factor I receptor gene on growth and transformation of mouse embryo fibroblasts. *Mol. Cell. Biol.* **14**, 3604–3612 (1994).
40. C. E. Tognon, M. J. Martin, A. Moradian, G. Trigo, B. Rotblat, S. W. G. Cheng, M. Pollard, E. Uy, C. Chow, J. M. Carboni, M. M. Gottardis, M. Pollak, G. B. Morin, P. H. B. Sorensen, A tripartite complex composed of ETV6-NTRK3, IRS1 and IGF1R is required for ETV6-NTRK3-mediated membrane localization and transformation. *Oncogene* **31**, 1334–1340 (2012).
41. S. Ahmed, X. Jin, M. Yagi, C. Yasuda, Y. Sato, S. Higashi, C. Y. Lin, R. B. Dickson, K. Miyazaki, Identification of membrane-bound serine proteinase matriptase as processing enzyme of insulin-like growth factor binding protein-related protein-1 (IGFBP-rP1/angiomodulin/mac25). *FEBS J.* **273**, 615–627 (2006).
42. A. R. Tee, C. G. Proud, Caspase cleavage of initiation factor 4E-binding protein 1 yields a dominant inhibitor of cap-dependent translation and reveals a novel regulatory motif. *Mol. Cell. Biol.* **22**, 1674–1683 (2002).
43. N. Wajapeyee, R. W. Serra, X. Zhu, M. Mahalingam, M. R. Green, Oncogenic BRAF induces senescence and apoptosis through pathways mediated by the secreted protein IGFBP7. *Cell* **132**, 363–374 (2008).
44. M. Wittman, J. Carboni, R. Attar, B. Balasubramanian, P. Balimane, P. Brassil, F. Beaulieu, C. Chang, W. Clarke, J. Dell, J. Eummer, D. Frennesson, M. Gottardis, A. Greer, S. Hansel, W. Hurlburt, B. Jacobson, S. Krishnananthan, F. Y. Lee, A. Li, T. A. Lin, P. Liu, C. Ouellet, X. Sang, M. G. Saulnier, K. Stoffan, Y. Sun, U. Velaparthi, H. Wong, Z. Yang, K. Zimmermann, M. Zoeckler, D. Vyas, Discovery of a (1*H*-benzoimidazol-2-yl)-1*H*-pyridin-2-one (BMS-536924) inhibitor of insulin-like growth factor I receptor kinase with in vivo antitumor activity. *J. Med. Chem.* **48**, 5639–5643 (2005).
45. D. Vasilcanu, A. Girnita, L. Girnita, R. Vasilcanu, M. Axelson, O. Larsson, The cyclolignan PPP induces activation loop-specific inhibition of tyrosine phosphorylation of the insulin-like growth factor-1 receptor. Link to the phosphatidyl inositol-3 kinase/Akt apoptotic pathway. *Oncogene* **23**, 7854–7862 (2004).
46. S. Mohseni-Zadeh, M. Binoux, Insulin-like growth factor (IGF) binding protein-3 interacts with the type 1 IGF receptor, reducing the affinity of the receptor for its ligand: An alternative mechanism in the regulation of IGF action. *Endocrinology* **138**, 5645–5648 (1997).
47. J. M. Ricort, M. Binoux, Insulin-like growth factor (IGF) binding protein-3 inhibits type 1 IGF receptor activation independently of its IGF binding affinity. *Endocrinology* **142**, 108–113 (2001).
48. C. Lalou, C. Lassarre, M. Binoux, A proteolytic fragment of insulin-like growth factor (IGF) binding protein-3 that fails to bind IGFs inhibits the mitogenic effects of IGF-I and insulin. *Endocrinology* **137**, 3206–3212 (1996).
49. J. Boucher, Y. Macotela, O. Bezy, M. A. Mori, K. Kriauciunas, C. R. Kahn, A kinase-independent role for unoccupied insulin and IGF-1 receptors in the control of apoptosis. *Sci. Signal.* **3**, ra87 (2010).
50. V. Evdokimova, P. Ruzanov, M. S. Anglesio, A. V. Sorokin, L. P. Ovchinnikov, J. Buckley, T. J. Triche, N. Sonenberg, P. H. B. Sorensen, Akt-mediated YB-1 phosphorylation activates translation of silent mRNA species. *Mol. Cell. Biol.* **26**, 277–292 (2006).

51. S. Qi, Y. Song, Y. Peng, H. Wang, H. Long, X. Yu, Z. Li, L. Fang, A. Wu, W. Luo, Y. Zhen, Y. Zhou, Y. Chen, C. Mai, Z. Liu, W. Fang, ZEB2 mediates multiple pathways regulating cell proliferation, migration, invasion, and apoptosis in glioma. *PLos One* **7**, e38842 (2012).
52. Y. Wang, P. Nangia-Makker, V. Balan, V. Hogan, A. Raz, Calpain activation through galectin-3 inhibition sensitizes prostate cancer cells to cisplatin treatment. *Cell Death Dis.* **1**, e101 (2010).
53. E. Agbottah, W. I. Yeh, R. Berro, Z. Klase, C. Pedati, K. Kehn-Hall, W. Wu, F. Kashanchi, Two specific drugs, BMS-345541 and purvalanol A induce apoptosis of HTLV-1 infected cells through inhibition of the NF-kappaB and cell cycle pathways. *AIDS Res. Ther.* **5**, 12 (2008).
54. Y. Zhuang, W. K. Miskimins, Metformin induces both caspase-dependent and poly (ADP-ribose) polymerase-dependent cell death in breast cancer cells. *Mol. Cancer Res.* **9**, 603–615 (2011).
55. J. Deng, T. Shimamura, S. Perera, N. E. Carlson, D. Cai, G. I. Shapiro, K. K. Wong, A. Letai, Proapoptotic BH3-only BCL-2 family protein BIM connects death signaling from epidermal growth factor receptor inhibition to the mitochondrion. *Cancer Res.* **67**, 11867–11875 (2007).
56. M. Toulany, T. A. Schickfluss, W. Eicheler, R. Kehlbach, B. Schittek, H. P. Rodemann, Impact of oncogenic *K-RAS* on YB-1 phosphorylation induced by ionizing radiation. *Breast Cancer Res.* **13**, R28 (2011).

Acknowledgments: We thank R. Baserga for providing Igf1r^{-} and IGF1R^{+} cells, Y. Amemiya for IGFBP7-expressing MDA-MB468 cells, A. Zhang for the help with FACS, P. Ari for densitometry, A. Evdokimov for statistical analysis, and J.-A. Chapman for helpful advice regarding statistical analysis. **Funding:** This work was supported by the Canadian Breast Cancer Research Alliance special program on metastasis and Canadian Institutes of Health Research (CIHR) grants to A.S. (MOP-97996) and to P.H.B.S. (MOP-119599). C.E.T. was funded through funds from the British Columbia Cancer Foundation through donations to P.H.B.S. from Team Finn and other generous riders in the Ride to Conquer Cancer. **Author contributions:** V.E. designed and performed the experiments, analyzed the data, and wrote the paper. C.E.T. performed immunohistochemistry staining, analyzed the data, and wrote the paper. T.B. and W.Y. cloned and purified truncated IGFBP7; performed mouse studies, immunohistochemistry, and FACS experiments; and made corrections to the manuscript. K.K. performed FACS experiments and analyzed the data. M.P., P.H.B.S., and A.S. analyzed the data and wrote the paper. **Competing interests:** The authors declare that they have no competing interests.